Comparison between Design Methods Applied to Segmental Tunnel Linings

N.A. Do[1,4*], D. Dias[2], P.P. Oreste[3], I. Djeran-Maigre[1]
[1]*Laboratory LGCIE, INSA of Lyon, University of Lyon, Villeurbanne, France*
[2]*Laboratory LTHE, Grenoble Alpes University, F-38000 Grenoble, France*
[3]*Department of Environmental, Land and Infrastructural Engineering, Politecnico di Torino, Italy*
[4]*Department of Underground and Mining Construction, Hanoi University of Mining and Geology, Vietnam*
[*]*E-mail*: nado1977bb@gmail.com

ABSTRACT: Development of the underground construction system in urban areas in Vietnam, such as Hanoi capital and Ho Chi Minh city, plays an important role to improve the public infrastructures. As most of the tunnels driven in urban areas using mechanized tunnelling method, segmental linings will be utilized in this project. One of the most important aspects during the design of a segmental tunnel lining is to consider the effect of segmental joints on its overall behaviour. This paper has the aim to introduce comparative results of calculated internal forces obtained by using analytical analyses, that is, Einstein & Schwartz's method, elastic equation method, and a two-dimensional numerical analysis, in which the effects of segmental joints have been taken into account. A cross-section of a twin bored tunnels of the Nhon - Hanoi Railway station section of the Hanoi pilot light metro has been used as a case studied.

KEYWORDS: Analytical method, Internal forces, Numerical method, Segmental lining, Tunnel.

1. INTRODUCTION

Application range of mechanized tunnelling method has been extended more and more. Segmental concrete linings are usually utilized to support these tunnels. The static action of the lining will be determined in a large measure by its rigidity, i.e., by its overall capacity to resist to deformation, the combined effect of the deformation of the segments and the one of the joints. In majority of the reinforced concrete precast linings, the deformation at the joints has a significant effect on the deformation of the segments. Thus, the magnitude and distribution of the internal forces depend to a great extent upon the distribution and characteristic of the joints. Consequently, one of the most important factors in designing a segmental tunnel lining is the influence of the segmental joints on its overall behaviour.

Many design methods for segmental lining have been developed and can be classified into three main groups including empirical methods, analytical methods and numerical methods (BTS 2004, Oreste 2007). Due to the simplicity, analytical methods are usually used for preliminary design purpose. Einstein & Schwartz (1979) proposed an analytical model to design tunnel lining on the basis of assuming plane condition, isotropic and homogenous elastic medium and elastic lining for a circular tunnel. Another method that is the elastic equation method was proposed in the Japanese Standard for Shield Tunnelling (JSCE 1996). This method is very simple to calculate internal forces of circular tunnels and has been widely used in Japan. In both above methods, the influence of the joints between segments is not taken directly into consideration through the existence of segmental joints in the calculation model. This influence is instead considered through a reduction factor applied to the bending rigidity of the lining.

Rapid progress in the development of user friendly computer codes and the limitations of analytical methods have led to an increase in the use of numerical methods for the design of tunnel lining. In comparison with analytical methods, numerical methods, especially three-dimensional (3D) numerical models, are obviously the only manner to take into consideration in a rigorous way the problem (Dias and Kastner 2000, Dias et al. 2000, Zheng-Rong et al. 2006, Oreste and Dias 2012, Oreste 2013, Mollon et al. 2013, Do et al. 2013c, Do et al. 2014c, Dias and Oreste 2013). However, due to their complexity and the time consuming, 3D numerical models seem to be only used in special underground works. Two-dimensional (2D) numerical analyses are therefore commonly used for the reason that they require less computer resources and time (Dias and Kastner 2013).

In this paper, comparisons of internal forces induced in a segmental tunnel lining determined using analytical analyses, that is, Einstein & Schwartz's method, elastic equation method as well as a 2D numerical analysis, have been conducted. A cross-section of a twin bored tunnels of the Nhon - Hanoi Railway station section of the Hanoi pilot light metro has been used as a case studied. The merits of the design methods are discussed.

2. THE CASE STUDIED: HANOI PILOT LIGHT METRO

The Nhon - Hanoi Railway station section of the Hanoi pilot light metro that is 12.5 km long is now under contracting stage. This section starts in the East suburban city of Nhon where the maintenance depot is located and will reach the Hanoi railways central station (Ga Ha Noi) in front of Tran Hung Dao avenue. The project comprises several types of infrastructures (see Figure 1) (MRB 2012). Firstly, a 8.5 km single track U-viaduct will be setup in urban areas, which helps to save considerably the construction costs. A 4 km tunnel, which has the aim to preserve the urban environment, will be constructed in the centre of the city. Twin horizontal tunnel solution has been chosen, which allow meeting the challenges of geological condition and minimizing the risk. Generally, two tunnels will be excavated in parallel at a distance of about 16 m from centre to centre. The external excavation diameter (D) of each tunnel is 6.3 m (MRB 2012).

In this study, for the purpose of comparing different calculation methods, a typical cross section is chosen. The twin tunnels are located at a depth of 21.7m below the ground surface (see Figure 2). Table 1 illustrated geo-mechanical properties of geological formations determined through extensive in situ and laboratory tests.

A precast concrete lining, in which each tunnel ring consists of 6 uniform segments corresponding to 6 segment joints that are assumed located at angles of 0^0, 60^0, 120^0, 180^0, 240^0, 300^0 measured counter-clockwise with respect to the right spring line, has been adopted. The structural design parameters of the tunnel lining are assumed as listed below:

Young's modulus $E_l = 35000$ MPa;

Poisson's ratio $\nu_l = 0.15$;

Lining thickness $t_l = 0.3$ m.

3. DESIGN METHODS

3.1. Einstein and Schwartz's method

Einstein & Schwartz (1979) use two ratios: the compressibility ratio C* and the flexibility ratio F* to take into account the interaction between the tunnel lining and the surrounding ground medium using symmetric loading conditions and anti-symmetric loading conditions, respectively.

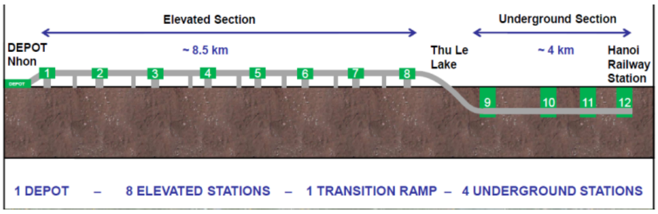

Figure 1 Pilot line Nhon - Hanoi Railway station (MRB 2012)

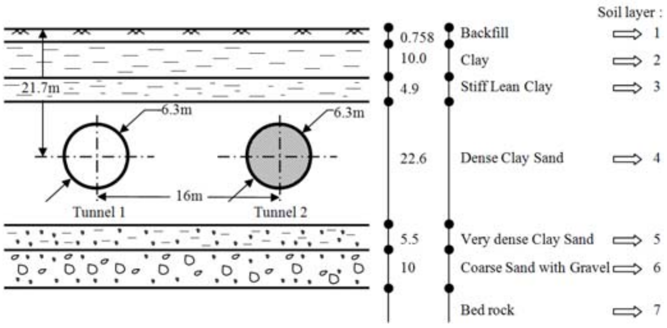

Figure 2 Geological conditions of considered section

Table 1 Geotechnical properties (MRB 2012)

Parameters/ Soil layer	Soil 1	Soil 2	Soil 3	Soil 4	Soil 5	Soil 6	Soil 7
Young's modulus E MPa)	1	2.8	5.2	10	10	150	15000
Poisson's ratio ν	0.42	0.39	0.37	0.31	0.3	0.28	0.35
Cohesion c (kPa)	5	5	25	0	0	0	200
Internal friction φ (degree)	15	20	25	34	35	37	45
Density γ (kN/m^3)	14	16	19	20	20	21	23
Earth coefficient at rest K_0	0.74	0.66	0.58	0.44	0.43	0.40	0.29

This method assumed that the ground surrounding the tunnel is homogeneous and isotropic. The results of bending moment (M) and normal force (N) are given considering with and without bonding forces between the tunnel lining and the ground. These two cases correspond to the no-slip case and the full-slip case as mentioned below. In this method, the value of bending moment and normal force are controlled by the flexibility ratio. For a large value of the flexibility ratio and the compressibility ratio (large deformation modulus of ground), the bending moment and normal force, respectively, become small and vice versa.

The internal forces for the no-slip case can be calculated using formulas (Einstein & Schwartz 1979):

$$\frac{N}{\sigma_v R} = \frac{1}{2}\left(1+K_0\right)\left(1-a_0^*\right)+\frac{1}{2}\left(1-K_0\right)\left(1+2a_2^*\right)\cos 2\theta \tag{1}$$

$$\frac{M}{\sigma_v R^2} = \frac{1}{4}\left(1-K_0\right)\left(1-2a_2^*+2b_2^*\right)\cos 2\theta \tag{2}$$

The internal forces for the full-slip case can be calculated using formulas (Einstein & Schwartz 1979):

$$\frac{N}{\sigma_v R} = \frac{1}{2}\left(1+K_0\right)\left(1-a_0^*\right)+\frac{1}{2}\left(1+K_0\right)\left(1-2a_2^*\right)\cos 2\theta \tag{3}$$

$$\frac{M}{\sigma_v R^2} = \frac{1}{2}\left(1-K_0\right)\left(1-2a_2^*\right)\cos 2\theta \tag{4}$$

where N is the normal force (MN), M is the bending moment (MN.m), θ is the angular location measured counter clockwise with respect to the right spring line (degree), R is the tunnel radius (m), σ_v is the vertical stress (MN/m^2), K_0 is the lateral earth pressure coefficient, E is the Young's modulus of the ground (MN/m^2), and a^*_0, a^*_2, b^*_2 are dimensionless coefficients (Figure 3).

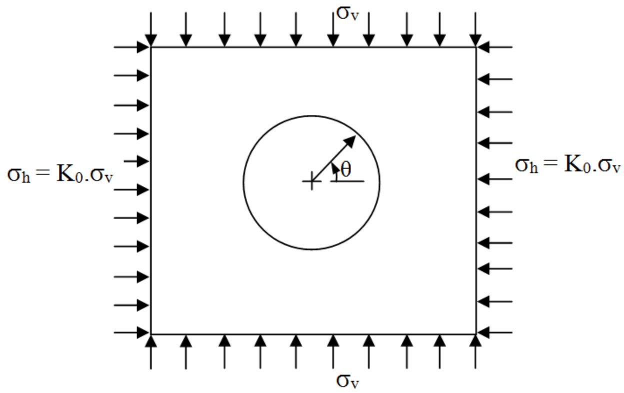

Figure 3 Geometry problem of the Einstein and Schwartz's method

The influence of the segmental lining joints is not considered directly in Einstein & Schwartz's method. A reduction factor, η, which could be determined using the effective moment of inertia of the overall lining proposed by Muir Wood (1975), has been instead applied to the bending rigidity (E_lJ_l):

$$\eta = \frac{\left(E_l J_l\right)_{eq}}{E_l J_l} \tag{5}$$

where $(E_lJ_l)_{eq}$ is the bending stiffness of a segmental lining with joints and E_lJ_l is the bending stiffness of a continuous lining without joints.

3.2. Elastic equation method

The elastic equation method (JSCE 1996) is a simple method which permits to calculate internal forces of circular tunnels. Loading distribution used for this method is shown in Figure 4. Like the Einstein and Schwartz's method, a reduction factor, η, has been applied to the bending stiffness of the segmental lining in order to take into consideration the effect of the joints.

In Figure 4, P_0 is the surcharge on the ground surface; R_0 is the external radius of the tunnel lining; R_c is the radius of the middle line of the tunnel lining; g is the gravity; P_{el} and P_{wl} are, respectively, the vertical earth pressure and the water pressure that act on the upper side of the tunnel lining. The lateral earth pressure and water pressure vary linearly and act on both sides of the tunnel lining. They are equal to q_{el} and q_{wl} at the top of the tunnel lining, and q_{e2} and q_{w2} at the bottom of the tunnel lining; P_{e2} and P_{w2} are respectively the vertical earth pressure and water pressure that act on the bottom side of the tunnel lining; P_g is the vertical resistance of lining weight that acts on the bottom side of the tunnel lining.

In the elastic equation method, the influence of the ground deformation modulus is defined by the subgrade reaction modulus k that can be determined by the formula proposed by AFTES (1993):

$k = E/(R_0*(1+\nu))$ in which R_0 is the external radius of tunnel and E and ν are, respectively, the Young's modulus and the Poisson's ratio of the ground. Elastic formulas for the calculation of internal forces used in this method are given in Table 2.

3.3. 2D numerical model

Numerical models have recently been used more and more to model bored tunnels supported by segmental lining (Dias et al. 2000, Dias and Kastner 2000, Dias and Kastner 2012, Do et al. 2013a, Do et al. 2013b, Do et al. 2013c, Do et al. 2014a, Do et al. 2014b). One of the main advantages of numerical models is their ability to simulate the joints between segments in a ring, interaction between the segmental lining and the soil surrounding tunnel.

Tunnelling process is in fact a 3D problem. Modelling this process in a 2D plane strain analysis requires a simplified assumption that allows 3D tunnelling effect to be taken into consideration. This assumption allows the pre-displacement of the ground surrounding the tunnel boundary, prior to the structural element installation, to be taken into account. This pre-displacement process of the tunnel boundary is hereafter called the de-confinement process. The works conducted by Karakus (2007) and Do et al. (2014a) indicated that the convergence-confinement method (CCM) (Panet 1982, Hejazi et al. 2008,), which has been adopted in this study, can be used efficiently for this purpose.

On the basis of numerical models that have been developed by the same authors (Do et al. 2013b, Do et al. 2013c, Do et al. 2014b), Figure 5 illustrates the two-dimensional numerical model assuming plane strain conditions that has been used to determine the internal forces induced in segmental lining in the present study.

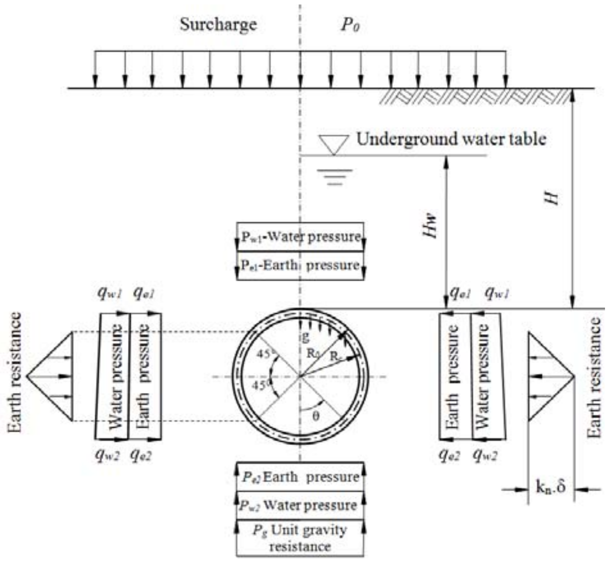

Figure 4 Load condition of Elastic Equation Method (JSCE 1996)

Table 1 Equations of internal forces for Elastic Equation Method (JSCE 1996)

Load	Bending moment	Axial Force	Shear Force
Vertical load $(P = p_{e1} + p_{w1})$	$(1\text{-}2S2).P.R_c^2/4$	$S2.R_c.P$	$\text{-}S.C.R_c.P$
Horizontal load $(Q = q_{e1} + q_{w1})$	$(1\text{-}2C2).Q.R_c^2/4$	$C2.R.Q$	$\text{-}S.C.R_c.Q$
Horizontal Triangular Load $(Q' = q_{e2} + q_{w2} - q_{e1} - q_{w1})$	$(6\text{-}3C\text{-}12C2+4C3).Q'.R_c^2/48$	$(C+8C2\text{-}4C3).Q'.R_c/16$	$(S+8S.C\text{-}4S.C2).Q'.R_c/16$
Soil Reaction $(P_k = k.\delta_h)$	$0 \le \theta \le \pi/4$ $(0.2346\text{-}0.3536C).R_c^2.k.\delta$ $\pi/4 \le \theta \le \pi$ $(-0.3487+0.5S2+ 0.2357C3).R_c^2.k.\delta$	$0 \le \theta \le \pi/4$ $0.3536C.R_c.k.\delta$ $\pi/4 \le \theta \le \pi$ $(-0.7071C+C2+ 0.7071S2C).R_c.k.\delta$	$0 \le \theta \le \pi/4$ $0.3536S.R_c.k.\delta$ $\pi/4 \le \theta \le \pi$ $(S.C\text{-}0.7071C2S).R_c.k.\delta$
Dead Load $(P_g=\pi.g)$	$0 \le \theta \le \pi/2$ $(3/8\pi\text{-}\theta.S\text{-}5/6C).R_c^2.g$ $\pi/2 \le \theta \le \pi$ $[-\pi/8+(\pi-\theta)S\text{-}5/6C\text{-}1/2\pi.S2].R_c^2.g$	$0 \le \theta \le \pi/2$ $(\theta.S\text{-}1/6C).R_c.g$ $\pi/2 \le \theta \le \pi$ $[-\pi.S+\theta.S+\pi.S2\text{-}1/6C].R_c.g$	$0 \le \theta \le \pi/2$ $(\theta.C\text{-}1/6S).R_c.g$ $\pi/2 \le \theta \le \pi$ $[-(\pi-\theta).C+\pi.S+\pi.S.C\text{-}1/6S].R_c.g$
Horizontal Deformation at Spring Line (δ_h)	$\delta_h = [(2P\text{-}Q')+\pi.g].R_c^4/[24.(E.I/h+0.045k.R_c^4)]$		

θ=angle from crown, S=sinθ, $S2= \sin^2\theta$, C=cosθ, $C2=\cos^2\theta$, $C3=\cos^3$

The numerical model is performed by means of the finite difference element program $FLAC^{3D}$ (Itasca 2009). The soil behaviour has been assumed to be governed by an elastic perfectly-plastic constitutive model, based on the Mohr-Coulomb failure criterion. The behaviour of the tunnel lining is assumed to be linear-elastic. The numerical analysis has been performed under drained conditions.

As described in the works of the same authors (Do et al. 2013a, Do et al. 2013b, Do et al. 2013c), embedded liner elements are attached to the zone faces along the tunnel boundary. The liner-zone interface stiffness (normal stiffness k_n and tangential stiffness k_s) is chosen using a rule-of-thumb in which k_n and k_s are set to one hundred times the equivalent stiffness of the stiffest neighbouring zone (Itasca 2009). The $FLAC^{3D}$ model grid contains a single layer of zones in the y-direction. The numerical model is 176 m wide in the x-direction, 71.75 m in the z-direction, which consists of approximately 14,260 zones and 28,712 grid points. The nodes were fixed in the directions perpendicular to the x-z and the y-z planes (i.e., y = 0, y = 1, x = -96 and x = 80), while the nodes at the base of the model (z = -50) were fixed in the vertical (z) direction (Figure 5).

The segment joints are simulated using a double node connection. As described by Do et al. (2013a), the axial stiffness of a segment joint has been represented by a linear relation. The radial stiffness and rotational stiffness of a segment joint have been modelled by means of a bi-linear relation that is characterized by a stiffness factor and a maximum bearing capacity. The values of the above spring stiffnesses used to simulate the segment joints have been determined on the basis of the normal forces, which act on the joint surface, using the simplified procedures presented by Thienert and Pulsfort (2011) and Do et al. (2013a). In this study, segment joints with rotational spring stiffness, maximum bending moment at segment joint, axial stiffness and radial stiffness of 100 MNm/rad/m, 150 kNm/m, 500 MN/m and 1050 MN/m, respectively, have been adopted. Other descriptions of the numerical model could be found in the works of the same authors (Do et al. 2013a, Do et al. 2013b, Do et al. 2013c, Do et al. 2014a).

Simulation of the construction process of tunnel has been carried out in the following phases:

- Phase 0 (model setup): the first step corresponds to the setup of the model, assignment of the plane strain boundary conditions (Figure 5) and the initial stress state, taking into consideration the influence of the gravity;
- Construction of the first tunnel, which includes three phases as follows (see Figure 6):
  - Phase 1 (de-confinement process): Deactivating the excavated ground and simultaneously applying a stress relaxation ratio λ_d of 0.3 (Möller and Vermeer 2005) to the excavation boundary.
  - Phase 2 (Injection process): Activating the segments in a lining ring on the tunnel boundary, assigning the joint's link conditions, simultaneously applying the total relaxation (λ_d = 1) and setting up the grouting pressure over the whole tunnel boundary on both tunnel structure and ground surface. The radial distribution of grouting pressure is assumed to linearly increase with depth due to the effect of grout unit weight. The grouting pressure applied at the tunnel crown is generally determined using the following formula (Mollon et al., 2013):

$$\sigma_{inj} = 1.2 \cdot \sigma_v \tag{6}$$

where σ_v is the soil overburden stress at the tunnel crown.

  - Phase 3 (consolidation process): The consolidation phase is simulated by removing grouting pressures that act on the ground and tunnel structure. The surrounding ground contacts to the lining structure through a solid grout layer of 15 cm with Young's modulus and unit weight of 10 MPa and 15 kN/m^3, respectively (Mollon et al. 2013, Do et al. 2013c).
- Starting the construction of the second tunnel using the same procedure applied to the first tunnel, which includes three phases ordered as phase 4, phase 5 and phase 6, respectively.

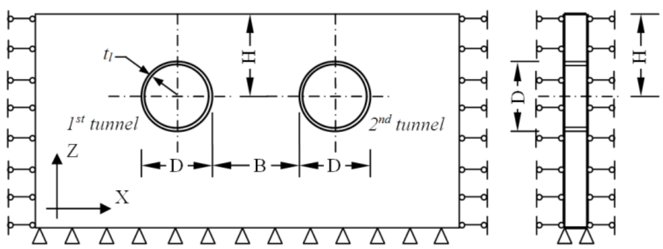

Figure 5 Plain strain model under consideration (not scaled)

4. RESULTS AND DISCUSSION

Table 3 presents the maximum bending moment and normal forces obtained from the Einstein and Schwartz's method, the elastic equation method and the 2D numerical model. The diagrams of the bending moment and normal forces developed in the tunnel lining are presented in Figure 7 and Figure 8, respectively. When using the numerical model, internal forces induced in the first tunnel are measured at phase 3, which correspond to those of a single tunnel, and at phase 6 in order to take into consideration the effect of the second tunnel construction on the existing tunnel. As far as the second tunnel is concerned, the internal forces in the tunnel lining are determined at phase 6.

For comparison purpose, the internal forces determined in the lining of the first tunnel at phase 3, which correspond to those of a single tunnel, are used as references. The results in Table 3 show that the maximum normal forces obtained in the two analytical methods are almost similar and are higher than that obtained with the numerical method. This could be attributed to the fact that, in the numerical model, the ground surrounding the tunnel not only causes the loads that act on the tunnel lining but also play an important role which helps to support the impact of further ground. This self-support capacity of the ground leads to a reduction in the ground loads that act on the tunnel lining. As a result, the normal forces obtained with the numerical method are lower than that determined by analytical methods. Furthermore, instead of using a staggered pattern of segment joints along the longitudinal axis of the tunnel, which is usually applied in reality, a straight pattern has been adopted in the 2D plane strain numerical model used in this study. A tunnel lining using straight pattern would result in smaller efforts (bending moment and normal forces) and in larger normal displacements compared to those of a tunnel supported by a staggered lining (Do et al. 2013c).

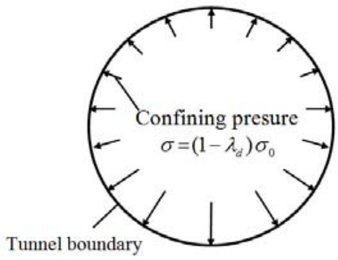

a) Phase 1: De-confinement process

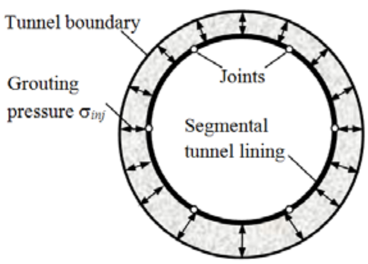

b) Phase 2: Grouting injection process

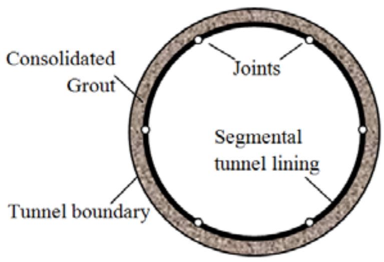

c) Phase 3: Grouting consolidation process

Figure 6 Excavation procedure of a tunnel

Table 3 Summary of analysis results

Parameters	Elastic equation method	Einstein and Schwartz's method		FLAC^{3D} numerical model		
				Tunnel 1		Tunnel 2
		Full-slip	No-slip	Phase 3 (*reference case*)	Phase 6	Phase 6
M (kN.m/m)	135	226	203	110	112	104
% M difference with the reference case	*22.7*	*105.5*	*84.5*	-	*1.8*	*-5.5*
N (kN/m)	680	694	709	591	647	606
% N difference with the reference case	*15.1*	*17.4*	*20.0*	-	*9.5*	*2.5*
Settlement (mm)	-	-	-	9.9	17.4	

(- no available in analytical methods)

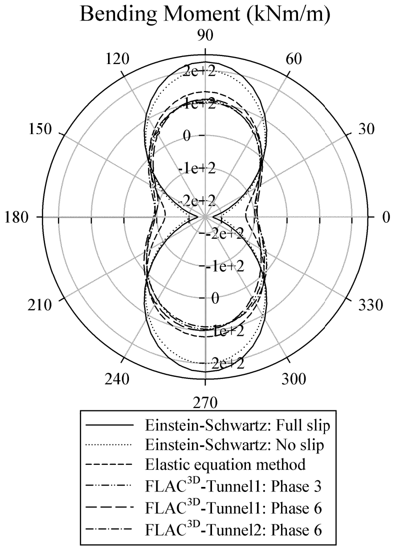

Figure 7 Bending moment diagram

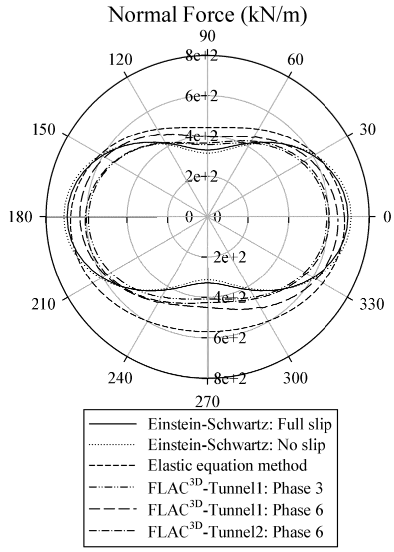

Figure 8 Normal forces diagram

The maximum bending moments obtained by Einstein and Schwartz in cases of full-slip and no-slip are 66.6% and 49.9%, respectively, higher than the one obtained by elastic equation method. It can be explained also by the low value of the deformation modulus of ground (E=10 MPa). Einst

ein and Schwartz's method is in fact very sensitive to the Young's modulus (E) value. Generally, the lower the Young's modulus of the ground, the larger the bending moment induced in tunnel lining. On the other hand, the deformation modulus only has an indirect influence on the tunnel lining through the reaction forces at the side walls in the elastic equation method. This indirect influence has a considerable impact on the lining internal forces.

As far as the numerical results are concerned, the shape of normal force diagram is more or less the same with the one obtained using the elastic equation method and both of them are significantly different from the one obtained with Einstein and Schwartz's method, especially at the bottom zone (see Figure 8). This difference can be explained by the increase in loads over the height of the tunnel wall under the influence of gravity, which is appropriate for shallow tunnels, considered in both the numerical model and the elastic equation method but not in analytical model proposed by Einstein and Schwartz. This may be also one of the main reasons for the difference in the shape of bending moment diagrams induced in the tunnel lining (Figure 7).

The numerical results also show that the internal forces in the first tunnel show slight increases of 1.8% and 9.5% in the bending moment and normal force, respectively, due to the impact of the excavation process of the second tunnel. These increases can be explained by the increase in vertical displacement above the first tunnel due to the impact of the second tunnel excavation as can be seen in Figure 9, which causes the development of vertical loads that act on the first tunnel. However, due to the distance between two tunnels of 2.5 D, which is quite large, the influence can be ignored. Indeed, the works conducted by Do et al. (2014b) indicated that when two tunnels are excavated in parallel, the impact between the two tunnels is considerable if the distance between the centres of two tunnels is smaller than two tunnel diameters. This is why the internal forces induced in the second tunnel are almost similar as those developed in a single tunnel (internal forces values observed at phase 3 in the first tunnel) (Table 3, Figure 7 and Figure 8).

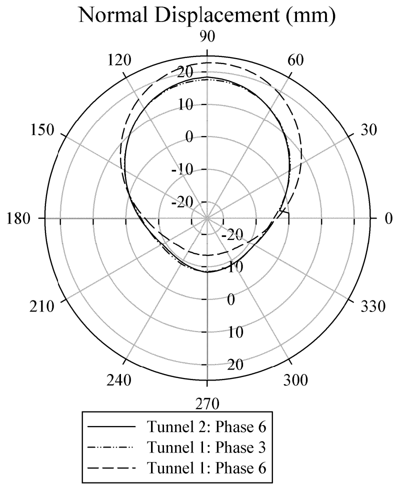

Figure 9 Normal displacement

The results in Figure 9 illustrate the normal displacements developed in the tunnel linings, in which the positive and negative values correspond to the inward and outward deformations of the tunnel lining. As expected, the excavation of the second tunnel causes increases inward deflections in the top-half region of the first tunnel. The maximum increase of about 30% is observed at the tunnel crown.

Apart from the advantage of allowing the designer to model construction sequences and consider the effect of soil structure interaction, one of the main advantages of numerical analysis compared to analytical methods is the ability to determine the deformation of ground surrounding the tunnel.

Figure 10 shows the development of the surface settlement trough in the transverse section during the excavation of twin tunnels. It can be seen that the twin tunnels cause an increase in the surface settlement. This could be explained by the accumulated loss of the ground in both two tunnels. In the considered case, the maximum settlement measured above the twin tunnels is 76 % higher than the one developed above a single tunnel.

Figure 10 also indicates that the two settlement troughs caused by the excavation of the tunnels on the left and right have similar shape and approximately the same maximum value. The settlement trough above the new tunnel (right) is determined on the basic of the final settlement trough of the twin tunnels minus the one developed above the existing tunnel (left) before it interacts with the new tunnel. The similarity of settlement troughs induced by the excavation of each tunnel could be attributed to the large distance between the two tunnels as mentioned above.

It is necessary to note that in the numerical model, all seven ground layers are simulated. However, the effects of some elements during the construction process (jacking force, etc) were not taken into account.

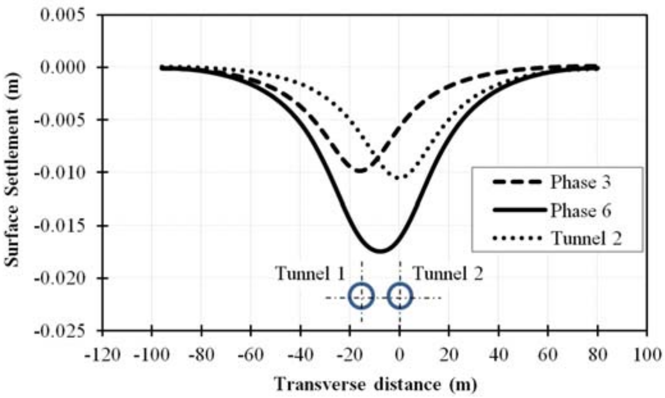

Figure 10 Surface Settlement

It is necessary to note that in the numerical model, all seven ground layers are simulated. However, the effects of some elements during the construction process (jacking force, etc) were not taken into account.

5. CONCLUSIONS

In this paper, comparative results of internal forces induced in segmental tunnel lining determined using Einstein & Schwartz's method, elastic equation method, and a 2D numerical model were presented. A cross section of twin bored tunnel lining design of the Hanoi pilot light metro, Nhon - Hanoi Railway station section has been adopted as a case studied.

The analyses pointed out some differences in the internal forces in terms of bending moments and normal forces determined by these methods. These differences could be attributed to the difference in loading schemes that act on the tunnel structure and the influence of the subgrade reaction along the tunnel boundary.

The main limitation of the Einstein & Schwartz's method is the fact that it can only take into account homogenous and isotropic grounds, and not complicated strata. In this method, the stiffness of the lining is considered as constant along the tunnel circumference. The elastic equation method proposed by JSCE (1996) is also limited to the fact that it can only be applied to a single ground layer.

Numerical analyses have the ability of considering the effect of joints in the lining ring, the interaction between the tunnel and the surrounding ground, the excavation of tunnel through multiple ground layers, and the effect of construction process, which are obviously more realistic compared to traditional analytical methods. Numerical analysis also allows estimating deformations of the tunnel structure and surrounding ground. However it is necessary to note that numerical analysis is time consuming. Analytical method can therefore utilized as preliminary design tool due to the fact that they give higher efforts in the structure

6. REFERENCES

AFTES - WG7 (1993) Considerations on the Usual Methods of Tunnel Lining Design. French Tunneling and Underground Engineering Association, Working Group No. 7 - Temporary Supports and Permanent Lining.

Dias, D. and Kastner, R. (2013). "Movements caused by the excavation of tunnels using face pressurized shields - Analysis of monitoring and numerical modelling results". Engineering Geology, 152, pp 17-25.

Dias, D. and Kastner, R. (2000). "Slurry shield tunnelling: Comparison between in situ data and three dimensional numerical simulations". Geotech-Year 27-30 Nov. 2000, Bangkok, Thailand.

Dias, D., Kastner, R. and Maghazi, M. (2000). "Three dimensional simulation of slurry shield tunnelling". Geotechnical Aspects of Underground Construction in Soft Ground, Kusakabe, Fujita and Miyazaki (eds.), Balkema, Rotterdam, pp 351-356.

Dias, D. and Oreste, P.P. (2013). "Key factors in the face stability analysis of shallow tunnels". American Journal of Applied Sciences, 10 (9), pp1025-1038.

Do. N.A., Dias, D, Oreste, P.P. and Djeran-Maigre, I. (2013a). "2D numerical investigation of segmental tunnel lining behaviour". Tunnelling and Underground Space Technology, 37, pp 115-127.

Do. N.A., Dias, D, Oreste, P.P. and Djeran-Maigre, I. (2013b). "3D modelling for mechanized tunnelling in soft ground - Influence of the constitutive model". American Journal of Applied Sciences, 10 (8), pp 863-875.

Do N.A., Dias D., Oreste P.P. and Djeran-Maigre I., (2013c). "Three-dimensional numerical simulation for mechanized tunnelling in soft ground: the influence of the joint pattern". Acta Geotechnica, in press, doi 10.1007/s11440-013-0279-7.

Do. N.A., Dias, D, Oreste, P.P. and Djeran-Maigre, I. (2014a). "2D Tunnel Numerical Investigation - The Influence of the Simplified Excavation Method on Tunnel Behaviour". Geotechnical and Geological Engineering, 32(1), pp 43-58, doi.10.1007/s10706-013-9690-y.

Do. N.A., Dias, D, Oreste, P.P. and Djeran-Maigre, I. (2014b). "2D numerical investigations of twin tunnel interaction". Geomechanics and Engineering, 6(3), pp 263-275, doi.org/10.12989/gae.2014.6.3.263.

Do. N.A., Dias, D, Oreste, P.P. and Djeran-Maigre, I. (2014c). "Three-dimensional Numerical Simulation of a Mechanized Twin Tunnels in Soft Ground". Tunnelling and Underground Space Technology, 42, pp 40-51.

Einstein, H.H. and Schwartz, C.W. (1979). "Simplified analysis for tunnel supports". Journal of the geotechnical engineering division, pp 499-517.

Hejazi, Y., Dias, D., Kastner, R. (2008), "Impact of constitutive models on the numerical analysis of underground constructions", Acta Geotechnica, 3, pp 251-258.

Itasca (2009). FLAC Fast Lagrangian Analysis of Continua, Version 4.0. User's manual.

JSCE. (1996). Japanese Standard for Shield Tunnelling, Japan Society of Civil Engineers, Tunnel Engineering Committee English Edition of the Japanese Standard for Tunneling, Subcommittee Japan Society of Civil Engineers, The third edition, Tokyo.

Karakus, M. (2007). "Appraising the methods accounting for 3D tunnelling effects in 2D plane strain FE analysis". Tunnelling and Underground Space Technology, 22, pp 47-56.

Möller, S.C. and Vermeer, P.A. (2005). "Prediction of settlements and internal forces in linings due to tunnelling". Fifth International Symposium on Geotechnical Aspects of Underground Construction in Soft Ground, Preprint Volume, Session 4, pp 141-149.

Mollon, G., Dias, D. and Soubra, A. (2013). "Probabilistic analyses of tunneling-induced ground movements". Acta Geotechnica, 8, pp 181-199.

Muir Wood A. (1975). "The circular tunnel in elastic ground". Géotechnique 25(1), pp 115-127.

Oreste, P.P. (2013). "Face stabilization of deep tunnels using longitudinal fibreglass dowels". Int. J. Rock Mechan. Min. Sci., 58, pp 127-140.

Oreste, P.P. and Dias, D. (2012). "Stabilisation of the excavation face in shallow tunnels using fibreglass dowels". Rock Mech Rock Eng, 45, pp 499-517.

Oreste, P.P. (2007). "A numerical approach to the hyperstatic reaction method for the dimensioning of tunnel supports". Tunnell. Underground space Technol., 22, pp 185-205.

Panet, M., Guenot, A. (1982), "Analysis of convergence behind the face of a tunnel", In: Proceedings of the International Symposium, Tunnelling-82, pp 187-204.

HaNoi Metropolitan Railway Management Board (MRB) (2012). Hanoi Pilot Light Metro Line 3, Section Nhon - Hanoi Railway Station - Technical Design of Underground Section - Line and Stations, Package number: HPLMLP/CP-03.

The British Tunnelling Society and The Institution of Civil Engineers (BTS) (2004). Tunnel lining design guide. Thomas Telford Publishing, ISBN: 0 7277 2986 1, London.

Thienert, C., & Pulsfort, M. (2011). "Segment design under consideration of the material used to fill the annular gap". Geomechanics and Tunnelling, 4, pp 665-679.

Zheng-Rong, H., Wei, Z., Jing-Hua, L., Jian, L. and Rui, J. (2006). "Three dimensional numerical modelling of shield tunnel lining". Tunnelling and Underground Space Technology 21(3-4), pp 434-434.